Quark-gluon plasma formation time and direct photons from heavy ion collisions

Fu-Ming Liu* and Sheng-Xu Liu
Key Laboratory of Quark and Lepton Physics (MoE) and Institute of Particle Physics, Central China Normal University, Wuhan 430079, China

(Received 1 January 2013; revised manuscript received 4 March 2014; published 13 March 2014)

We investigated the information carried by the data on direct photons, i.e., the transverse momentum spectrum and the elliptic flow v_2 from Pb + Pb collisions at $\sqrt{s_{NN}} = 2.76$ TeV measured at the Large Hadron Collider and from Au + Au collisions at $\sqrt{s_{NN}} = 200$ GeV measured at the Relativistic Heavy Ion Collider, in the framework of (3 + 1)–dimensional ideal hydrodynamical models constrained with hadronic data. We found that these direct photon data may serve as a useful clock at the early stage of heavy ion collisions. The time scales for reaching thermal and chemical equilibrium, extracted from those data, are about 1/3 and 1.5 fm/c, respectively. Thus the large elliptic flow of direct photons is explainable. High-order harmonics, i.e., v_3, v_4, and v_5, of direct photons from Pb + Pb collisions at 2.76 TeV are also predicted, as a further test to compete with those who claim new sources of photons to account for the large elliptic flow of direct photons.

DOI: 10.1103/PhysRevC.89.034906 PACS number(s): 25.75.Cj, 12.38.Mh, 24.10.Nz, 25.20.Lj

I. INTRODUCTION

Recently, a large elliptic flow of direct photons, as large as that of hadrons, has been observed in heavy ion collisions, in both a PHENIX experiment at the Relativistic Heavy Ion Collider (RHIC) and an ALICE experiment at the Large Hadron Collider (LHC) [1,2]. Such a large elliptic flow of direct photons seems puzzling because the elliptic flow of direct photons was predicted to be much lower than that of hadrons [3–6].

New sources of direct photons [7,8] have been considered to account for the large elliptic flow. They should, on one hand, be constrained by the observed transverse momentum spectra of direct photons [2,9] and hadronic data and, on the other hand, be tested by higher order harmonics, for example, the triangular flow v_3 of direct photons.

In this paper, we investigate the special information carried by direct photons, after being constrained by the data on hadrons in heavy ion experiments. We try to explain direct photon data by the delayed formation of quark-gluon plasma (QGP) in the early stage, following some early suggestions of two time scales for thermal and chemical equilibrium [10–12]. Thus the QGP formation time $\tau_{\rm QGP}$, the moment when the system reaches both thermal and chemical equilibrium locally, will be extracted. In order to make the calculation of direct photons constrained by hadronic data, we take (3 + 1)–dimensional ideal hydrodynamical models [13,14], which can give a reasonable description of hadronic data such as rapidity distribution, transverse momentum spectra, and elliptic flow. More than one hydro model is employed, in order to make our conclusions more general. Throughout the calculation of direct photons, we keep the solutions from those hydro models valid and keep the equation of states consistent.

The paper is organized as follows: after a brief introduction of the calculation approach for direct photons in Sec. II, the results are presented in Sec. III, and the conclusion is given in Sec. IV.

*liufm@iopp.ccnu.edu.cn

II. CALCULATION APPROACH

We consider direct photons from PbPb collisions at 2.76 TeV and AuAu collisions at 200 GeV. The sources of direct photons are simplified as prompt photons and thermal photons, according to ALICE and PHENIX measurements of direct photons at a high transverse momentum [2,9]. Prompt photons are calculated to the next-to-leading order contribution in cold nuclear collisions,

$$\frac{dN^{\rm P}}{dyd^2p_{\rm t}} = T_{AB}(b)\sum_{ab}\int dx_a dx_b G_a(x_a,M^2)G_b(x_b,M^2) \times \frac{\hat{s}}{\pi}\delta(\hat{s}+\hat{t}+\hat{u})\left[\frac{d\sigma}{d\hat{t}}(ab\to\gamma+X) + K\sum_c \frac{d\sigma}{d\hat{t}}(ab\to cd)\int dz_c \frac{1}{z_c^2}D_{\gamma/c}(z_c,Q^2)\right], \tag{1}$$

where the thickness function $T_{AB}(b)$, nuclear parton distribution functions $G(x,M^2)$, and cross sections are the same as in previous work [15,16]. Energy loss in fragmentation functions $D_{\gamma/c}(z_c,Q^2)$ was not considered, in order to compensate the contribution from jet photon conversions. Prompt photons are supposed to carry a vanishing elliptic flow.

The $p_{\rm t}$ spectrum of thermal photons reads

$$\frac{dN^{\rm T}}{dyd^2p_{\rm t}} = \int d^4x\Gamma(E^*,T), \tag{2}$$

where $\Gamma(E^*,T)$ is the photon emission rate at temperature T and $E^* = p^\mu u_\mu$, p^μ is the four-momentum of a photon in the laboratory frame, and u_μ is the flow velocity.

The hydrodynamical models [13,14] provide us the energy density ϵ and flow velocity u_μ at each space-time point of the system for the calculation. We get the temperature at each space point according to the equation of state $\epsilon = \epsilon(T)$. We keep these solutions from hydro models valid all the time. However, the photon emission rate may be modified.

Now we introduce the two time scales in heavy ion collisions and discuss how photon emission depends on them. The hydrodynamical description of the heavy ion systems starts at an initial time τ_0, where a local thermal equilibrium has been assumed to solve the hydro equations. The high energy density at τ_0 ensures a partonic phase. The ratio between quarks and gluons at τ_0 cannot be determined by hadronic data. It takes time for the system to reach chemical equilibrium, thus a QGP may form at a later moment, $\tau_{\rm QGP}$, not at τ_0.

Quark fugacity ξ is used during $(\tau_0, \tau_{\rm QGP})$. A linear increase in the quark fugacity ξ from 0 at τ_0 to unity at $\tau_{\rm QGP}$ is assumed in this work. The assumption of $\xi = 0$ until τ_0 is, on one hand required by the large elliptic flow of direct photons and, on the other hand, reasonable with both CGC and EPOS initial conditions.[1]

Therefore, during $(\tau_0, \tau_{\rm QGP})$, the photon emission rate is not the full rate in the QGP phase $\Gamma_{\rm AMY}$ [17]. Contributions from the Compton process and annihilation processes, $\Gamma_{\rm Compton}$ and $\Gamma_{\rm annihilation}$ [18], should be modified by a factor of ξ and ξ^2, respectively. The Bremsstrahlung process with n quark lines will be modified by a factor of ξ^n, where $n \geqslant 2$. It is difficult to disentangle the contribution of a given n-quark Bremsstrahlung. Therefore we can either ignore Bremsstrahlung contributions to get the lower limit, $\Gamma^{\rm low}$, or overestimate them with $n = 2$. Thus, during $(\tau_0, \tau_{\rm QGP})$ the photon emission rate satisfies $\Gamma^{\rm low} < \Gamma < \Gamma^{\rm up}$, with the lower limit

$$\Gamma^{\rm low} = \xi \cdot \Gamma_{\rm Compton} + \xi^2 \cdot \Gamma_{\rm annihilation} \tag{3}$$

and the upper limit

$$\Gamma^{\rm up} = \xi \cdot \Gamma_{\rm Compton} + \xi^2 \cdot (\Gamma_{\rm AMY} - \Gamma_{\rm Compton}). \tag{4}$$

During this stage, there is also a modification of the relation $\epsilon = \epsilon(T)$ via

$$\epsilon = (d_g + \xi d_q)\frac{\pi^2}{30}T^4, \tag{5}$$

where the partonic degrees of freedom $d_g = 16$ and $d_q = 31.5$, and a certain increase in the temperature, especially at very small ξ. But the relation between energy density and pressure remains approximately, so that hydro solutions remain valid.

Now let us summarize photon emission throughout the evolution history:

(i) At $\tau = 0$, prompt photons are counted according to the next-to-leading-order QCD.
(ii) At $0 < \tau \leqslant \tau_0$, we have $\xi = 0$ and photon emission rate $\Gamma = 0$.
(iii) At $\tau_0 < \tau < \tau_{\rm QGP}$, emission is estimated with $\Gamma^{\rm low} < \Gamma < \Gamma^{\rm up}$.
(iv) For $\tau \geqslant \tau_{\rm QGP}$, the thermal photon emission rate covers the contributions from both the QGP phase and the hadronic phase. In the QGP phase, $\Gamma_{\rm AMY}$ is employed. In the hadronic phase, the rate is based on massive Yang-Mills theory [19], which takes into account both nonstrange and strange hadronic interactions such as $\pi + \rho \to \pi + \gamma$, $\pi + \pi \to \rho + \gamma$, and $\pi + K^* \to K + \gamma$.

The large elliptic flow of direct photons implies a strong emission in the hadronic phase. Therefore, we do not include the dipole-like form factor in the emission rate as done in most work [15,19]. This is favored not only by direct photon data, but also because the form factors of hadrons in strong interactions, and the PDF of these hadrons, have not been measured. Massive Yang-Mills theory itself remains complete without form factors.

Now we introduce the calculation of high-order harmonics. The $p_{\rm t}$ spectrum of thermal photons can be decomposed into harmonics of the azimuthal angle ϕ as

$$\frac{dN}{d\phi} \sim 1 + 2v_2\cos(\phi - \psi_2) + 2v_3\cos(\phi - \psi_3) + \cdots, \tag{6}$$

[1]Describing the nonequilibrium system at the early stage is a hot and challenging question in relativistic heavy ion physics. The space-time evolution of quark fugacity should be determined accordingly. Here we estimate quark fugacity at τ_0 according to the initial conditions. The initial conditions can be obtained from the Glauber model [14], according to the distribution of nucleons in nuclei, but it is difficult to extract the quark fugacity. The color glass condensate (CGC) model provides the initial conditions according to the parton distribution functions [21]. The small-x physics supports a glue-dominant system and $\xi \to 0$. The event generator EPOS [13] can provide the initial conditions based on the parallel exchange of pomerons, a kind of color tube with vacuum quantum numbers. The longitudinal excited color tubes easily accommodate gluons, which implies $\xi \to 0$ at midrapidity.

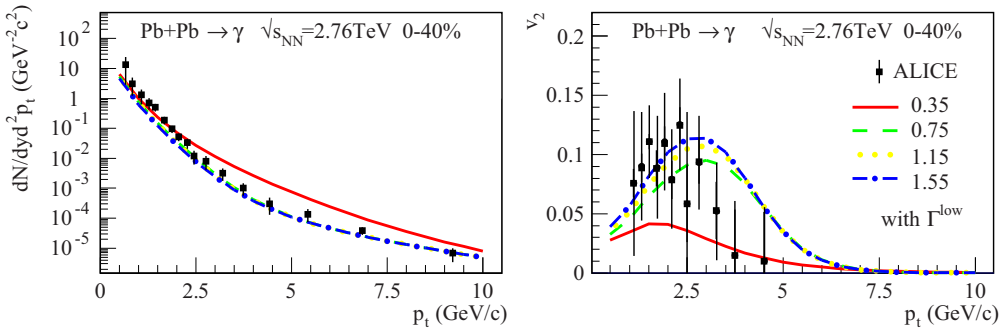

FIG. 1. (Color online) Transverse momentum spectrum and elliptic flow v_2 of direct photons from Pb + Pb collisions at $\sqrt{s_{NN}} = 2.76$ TeV for centrality 0–40%, calculated with $\tau_{\rm QGP} = 0.35$, 0.75, 1.15, and 1.55 fm/c. Data points from ALICE [2].

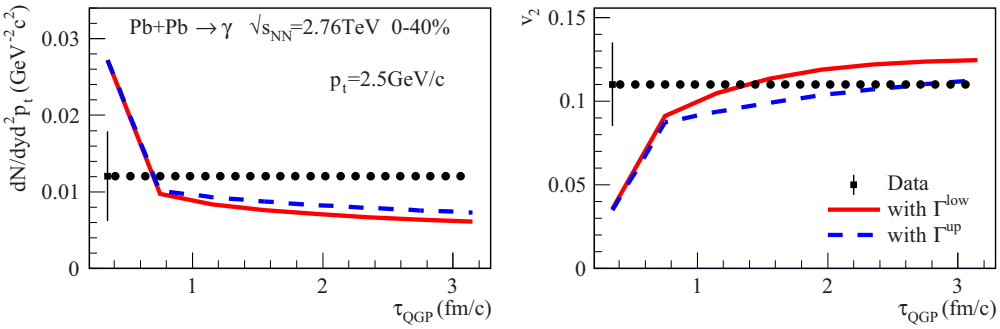

FIG. 2. (Color online) The dependence of the transverse momentum spectrum and elliptic flow v_2 on $\tau_{\rm QGP}$ are shown at $p_{\rm t} = 2.5$ GeV, where dashed lines and solid lines represent calculations with up and low limits, respectively, between τ_0 and $\tau_{\rm QGP}$. Data points are extracted from ALICE data [2] and horizontal lines are guides for the eye.

where v_2 (v_n) is the elliptic flow (higher order harmonics), and ψ_n is the nth-order event plane. Obviously, v_n and ψ_n depend on the photon's transverse momentum $p_{\rm t}$ and vary event by event. From Eq. (6), one can easily get

$$v_n \cos n\phi = \frac{1}{N}\int_0^{2\pi} \cos n\phi \frac{dN}{d\phi} d\phi,$$
$$v_n \sin n\phi = \frac{1}{N}\int_0^{2\pi} \sin n\phi \frac{dN}{d\phi} d\phi. \quad (7)$$

Let us note their right sides as $\langle \cos n\phi \rangle$ and $\langle \sin n\phi \rangle$, respectively. Then in each event one can estimate

$$v_n = \sqrt{\langle \cos n\phi \rangle^2 + \langle \sin n\phi \rangle^2}, \quad (8)$$

find the event average to get the v_n of thermal photons, and reduce by the factor $\frac{dN^{\rm T}/dp_t}{dN^{\rm T}/dp_t + dN^{\rm P}/dp_t}$ to get the v_n of direct photons.

III. RESULTS

A. An event-by-event calculation of direct photons from Pb + Pb collisions at $\sqrt{s_{NN}} = 2.76$ TeV

Let us start with Pb + Pb collisions at $\sqrt{s_{NN}} = 2.76$ TeV. Event-by-event thermal photon emission has been calculated based on EPOS2.17 v3 [13], where the initial time $\tau_0 = 0.35$ fm/c.

In Fig. 1, the transverse momentum spectrum and elliptic flow v_2 of direct photons from Pb + Pb collisions at centrality 0–40% calculated with $\tau_{\rm QGP} = 0.35, 0.75, 1.15$, and 1.55 fm/c are compared with the ALICE data [2]. At $\tau_0 < \tau < \tau_{\rm QGP}$, the lower emission limit was used for the curves.

Figure 1 shows that if QGP is formed at the initial time τ_0, then direct photons will be overproduced, and the elliptic flow underestimated. The underestimation of elliptic flow is consistent with previous work [3–6].

Delayed QGP formation will decrease the early photon emission and, thus, increase the elliptic flow of direct photons, shown in Fig. 1. The reason for this is clear. Later-emitted photons carry a larger elliptic flow, thanks to the longer expansion of the system. Once we reduce the fraction of early emission via the delayed QGP formation time, the total elliptic flow will increase.

The dependence of the transverse momentum spectrum and elliptic flow v_2 of direct photons on $\tau_{\rm QGP}$ is shown more clearly in Fig. 2. The rate at $\tau_0 < \tau < \tau_{\rm QGP}$ is not known explicitly, but the uncertainty is constrained by the upper (dashed lines) and lower (solid lines) limits. Here $p_{\rm t} = 2.5$ GeV/c are chosen to present the results, because both the transverse momentum spectrum and the elliptic flow show sensitivity to $\tau_{\rm QGP}$ here. Besides, the elliptic flow v_2 has a peak close to 2.5 GeV/c.

We can see that delayed QGP formation can increase the elliptic flow of direct photons and, at the same time, can decrease the transverse momentum spectrum. Now the direct photon data, extracted from ALICE data [2] and shown as filled black squares, are used to extract the proper QGP formation time. And a reasonable choice of $\tau_{\rm QGP}$ is about 1.5 fm/c.

The rate at $\tau_0 < \tau < \tau_{\rm QGP}$ is not known explicitly, but the uncertainty makes a theoretic error of less than 10% for both the spectrum and the elliptic flow of direct photons. In the following, we do not mention it but use the low limit of the emission rate directly.

In Fig. 3, the harmonics coefficients v_n ($n = 2, 3, 4, 5$) of direct photons are predicted with $\tau_{\rm QGP} = 1.55$ fm/c, accompanied by the ALICE data points for elliptic flow v_2. They behave quite similarly to those of the charged hadrons measured by ATLAS [20]. Thus the two-time-scale picture seems more reasonable than new sources of direct photons to account for the large elliptic flow.

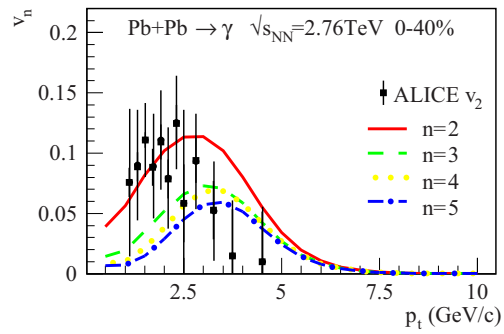

FIG. 3. (Color online) Predicted harmonics coefficients v_n ($n = 2, 3, 4, 5$) of direct photons are shown by various curves. Filled black squares are measured v_2 values [2].

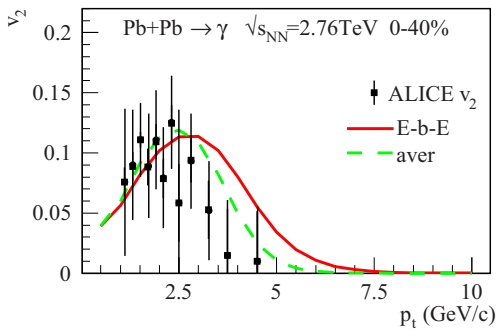

FIG. 4. (Color online) Elliptic flow of direct photons based on event-by-event and averaged calculations. Filled squares are measured v_2 values [2].

B. A connection between event-by-event and event-averaged calculations

In the above case, each system expands hydrodynamically based on an irregular initial condition and thermal photons are emitted event by event. Here we make a connection to an event-averaged calculation. The latter has a smoothed initial condition, almond-like in the transverse plane. This can be obtained from the average of the event-by-event initial conditions, with $\psi_2 = 0$ for each event, or parameterized with the Glauber model. The regular system expands hydrodynamically and emits photons, similarly to we did previously [6].

In Fig. 4, the elliptic flow of direct photons from the averaged calculation [dashed (green) line] is compared to that from the event-by-event calculation [solid (red) line]. The same maxima of elliptic flow are obtained, for both the event-by-event and the averaged calculation. But the high-order harmonics such as v_3, v_4, and v_5 vanish in the averaged calculation because of mixing of the irregular events.

The event-by-event curve moves leftward to reach the averaged curve. Further movement is needed to reach the data shape. As we know that viscosity plays a more important role for irregular systems, we may attribute the deviation from data shape to the lack of viscosity in the ideal hydrodynamics.

C. Direct photons from Au + Au collisions at $\sqrt{s_{NN}} = 200$ GeV

The correct choice of τ_0 is also important to get a large elliptic flow. $\tau_0 = 0.35$ fm/c is provided directly above. Various τ_0 values should be checked, but they are not available if we require a good reproduction of hadronic data. One available case is $\tau_0 = 0.6$ fm/c, as in our previous work [15], for Au + Au collisions at $\sqrt{s_{NN}} = 200$ GeV. This is a (3 + 1)–dimensional ideal hydrodynamics [14] with Glauber initial conditions. The averaged EPOS initial condition with $\tau_0 = 0.6$ fm/c provides the same elliptic flow at midrapidity [6] but a different rapidity dependence. So the following midrapidity discussion is general, valid for both of the two models.

In Fig. 5, the transverse momentum spectrum and elliptic flow v_2 of direct photons from Au + Au collisions at $\sqrt{s_{NN}} =$ 200 GeV for centrality 0–20% and 20%–40%, calculated with $\tau_{QGP} = 0.6$, 1.1, 1.6, 2.1, and 2.6 fm/c, are compared with PHENIX data points [1,9]. The previous results with hadronic form factors [15] (dashed lines) are very close to those calculated without form factors (solid lines), because the spectrum at high p_t is dominant by prompt photons, while at low p_t, form factors are close to unity.

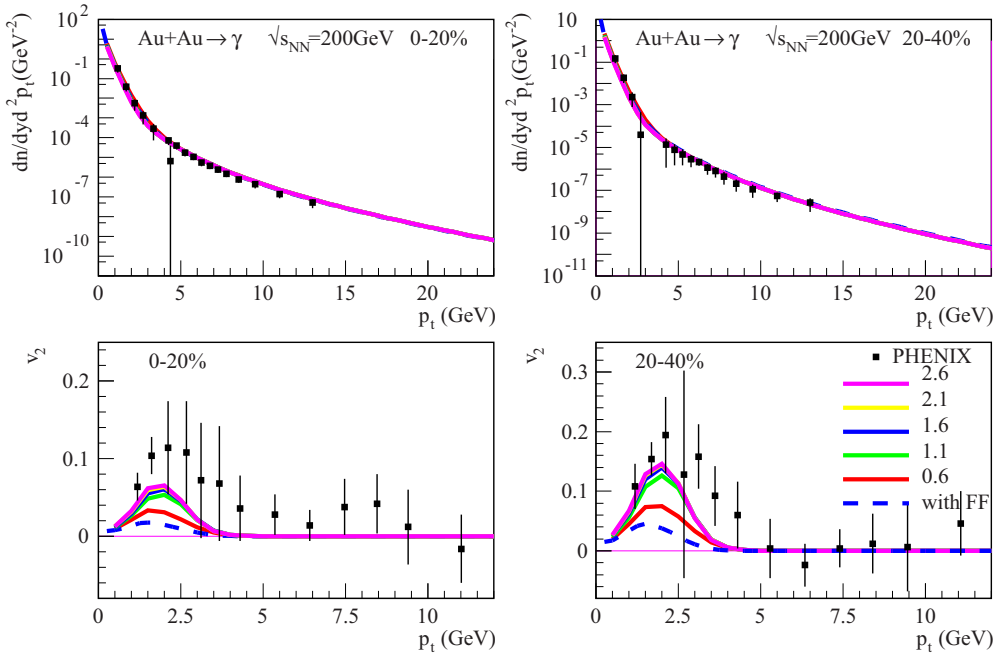

FIG. 5. (Color online) Transverse momentum spectrum and elliptic flow v_2 of direct photons from Au + Au collisions at $\sqrt{s_{NN}} = 200$ GeV for centrality 0–20% and 20%–40%, calculated with $\tau_{QGP} = 0.6$, 1.1, 1.6, 2.1, and 2.6 fm/c. The spectrum is not very sensitive to τ_{QGP}. The elliptic flow increases with τ_{QGP}, then saturates. Data points from PHENIX [1,9].

The solid curves overlap in the upper panels, which shows the insensitivity of the spectrum to $\tau_{\rm QGP}$. In the lower panels, the solid curves, from bottom to top, are calculated with $\tau_{\rm QGP} = 0.6$, 1.1, 1.6, 2.1, and 2.6 fm/c, respectively. The elliptic flow first increases with $\tau_{\rm QGP}$, then saturates. At $p_{\rm t} = 2$ GeV/c, the maximum of elliptic flow is only 60% of the measured value, for both centralities. Thus, $\tau_0 = 0.6$ fm/c cannot work.

IV. DISCUSSION AND CONCLUSION

The large elliptic flow and the transverse spectrum of direct photons from Pb + Pb collisions at $\sqrt{s_{NN}} = 2.76$ TeV have been explained with $\tau_0 \sim 1/3$ fm/c and $\tau_{\rm QGP} \sim 1.5$ fm/c. High-order harmonics coefficients such as v_3, v_4, and v_5 of direct photons have been predicted, and they also behave quite similarly to these variables for charged hadrons.

$\tau_{\rm QGP}$ has been studied systematically in this work. The test of τ_0 was done with two values, 0.35 and 0.6 fm/c. At $\tau_0 = 0.6$ fm/c, the large elliptic flow of direct photons from Au + Au collisions at $\sqrt{s_{NN}} = 200$ GeV cannot be fully reproduced. A delayed QGP formation time can make the elliptic flow larger, but only up to 60% of the measured value.

More work should be done systematically to extract τ_0 and $\tau_{\rm QGP}$ with systems such as AA, pA, and pp. A full explanation of the data for both charged hadrons and direct photons at both colliders is expected.

ACKNOWLEDGMENTS

F.M.L. thanks K. Werner and T. Hirano for providing the hydrodynamical evolution of two collision systems and U. Heinz, L. Mclarran, Y. Schutz, E. Shuryak, and K. Werner for very helpful discussions. This work was supported by the Natural Science Foundation of China under Project No. 11275081 and by the Program for New Century Excellent Talents in University (NCET).

[1] A. Adare *et al.* (PHENIX Collaboration), Phys. Rev. Lett. **109**, 122302 (2012).
[2] D. Lohner (ALICE Collaboration), J. Phys.: Conf. Ser. **446**, 012028 (2013).
[3] H. van Hees, C. Gale, and R. Rapp, Phys. Rev. C **84**, 054906 (2011).
[4] R. Chatterjee, H. Holopainen, I. Helenius, T. Renk, and K. J. Eskola, arXiv:1305.6443 [hep-ph].
[5] R. Chatterjee, E. S. Frodermann, U. W. Heinz, and D. K. Srivastava, Phys. Rev. Lett. **96**, 202302 (2006).
[6] F.-M. Liu, T. Hirano, K. Werner, and Y. Zhu, Phys. Rev. C **80**, 034905 (2009).
[7] G. Başar, D. E. Kharzeev, and V. Skokov, Phys. Rev. Lett. **109**, 202303 (2012).
[8] A. Bzdak and V. Skokov, Phys. Rev. Lett. **110**, 192301 (2013).
[9] S. Afanasiev *et al.* (PHENIX Collaboration), Phys. Rev. Lett. **109**, 152302 (2012).
[10] T. S. Biro, E. van Doorn, B. Muller, M. H. Thoma, and X. N. Wang, Phys. Rev. C **48**, 1275 (1993).
[11] E. Shuryak, Phys. Rev. Lett. **68**, 3270 (1992).
[12] E. Shuryak and L. Xiong, Phys. Rev. Lett. **70**, 2241 (1993).
[13] K. Werner, I. Karpenko, M. Bleicher, T. Pierog, and S. Porteboeuf-Houssais, Phys. Rev. C **85**, 064907 (2012).
[14] T. Hirano, U. Heinz, D. Kharzeev, R. Lacey, and Y. Nara, Phys. Lett. B **636**, 299 (2006); J. Phys. G **34**, S879 (2007); Phys. Rev. C **77**, 044909 (2008).
[15] F.-M. Liu, T. Hirano, K. Werner, and Y. Zhu, Phys. Rev. C **79**, 014905 (2009).
[16] F.-M. Liu and K. Werner, Phys. Rev. Lett. **106**, 242301 (2011).
[17] P. Arnold, G. D. Moore, and L. G. Yaffe, J. High Energy Phys. 11 (2001) 057; 12 (2001) 009.
[18] J. Kapusta, P. Lichard, and D. Seibert, Phys. Rev. D **44**, 2774 (1991); **47**, 4171(E) (1993).
[19] S. Turbide, R. Rapp, and C. Gale, Phys. Rev. C **69**, 014903 (2004).
[20] G. Aad *et al.* (ATLAS Collaboration), Phys. Rev. C **86**, 014907 (2012).
[21] F. Gelis, E. Iancu, J. Jalilian-Marian, and R. Venugopalan, Annu. Rev. Nucl. Part. Sci. **60**, 463 (2010).